DALTON
FULL PAPER

Exchange coupling in a bis(heterodinuclear) $[Cu^{II}Ni^{II}]_2$ and a linear heterotrinuclear complex $Co^{III}Cu^{II}Ni^{II}$. Synthesis, structures and properties

Cláudio Nazari Verani, Eva Rentschler, Thomas Weyhermüller, Eckhard Bill and Phalguni Chaudhuri *

Max-Planck-Institut für Strahlenchemie, Stiftstraße 34-36, D-45470 Mülheim an der Ruhr, Germany. E-mail: chaudh@mpi-muelheim.mpg.de

Received 22nd October 1999, Accepted 3rd December 1999

Two heterometallic complexes $[\{Cu^{II}(HLOX)Ni^{II}(N_3)\}_2]$ and $[(tmtacn)Co^{III}(\mu\text{-}OH)Cu^{II}(LOX)Ni^{II}(OH_2)_2][ClO_4]_2$ (tmtacn = 1,4,7-trimethyl-1,4,7-triazacyclononane) containing the same $[Cu^{II}Ni^{II}]$ core embedded in an unsymmetrical dicompartmental imine-oxime ligand H_4LOX have been synthesized and characterized. Their crystal structures show that the Cu^{II} resides at the $N(oxime)_2O(phenolate)_2$ site and assumes a planar geometry. The Ni^{II} is six-co-ordinated and bound to an N_2O_4 donor array comprising two iminonitrogens, two phenolate oxygens and two axially co-ordinated H_2O molecules. The cobalt(III) is low spin and six-co-ordinated. In DMF solution at 10 K the EPR spectra of the complexes exhibit a spin-doublet ground state with "inverted" g values which demonstrate the delocalization of the unpaired electron over the CuNi core. Magnetic susceptibility measurements over the range 2–290 K confirm that the paramagnetic nickel(II) and copper(II) centres are antiferromagnetically coupled, with values for the exchange coupling constant J through the phenolate oxygens of -115 cm^{-1} and -130 cm^{-1} respectively. Considering the dimer as a single tetranuclear unit, the coupling constant J' through the path Cu–N–O–Ni is very small ($\approx$1 cm^{-1}) but positive (ferromagnetic coupling).

Introduction

Exchange-coupled polynuclear complexes,[1–7] particularly heterometallic systems,[4–6] are of special interest due to their relevance to different branches of natural sciences, physics, chemistry and biology. There is an impressive diversity of spin-coupled structures in biology,[8,9] *e.g.* dicopper sites in hemocyanin and tyrosinase, diiron(III) sites in methemerythrin, ribonucleotide reductase, and heterobimetallic sites of Fe^{III} and Cu^{II} in respiratory cytochrome oxidase which catalyses the 4e reduction of dioxygen to water in the mitochondria of eukaryotic cells. Active sites involving more than one metal centre in metalloproteins have elicited the interest of bioinorganic chemists in such interactions. In another area of research the intimate relationship between spin coupling and molecular structure has fostered the emergence of molecular magnetism[2–4] as a multidisciplinary field. The fundamental understanding regarding the factors that determine the spin states of polynuclear transition metal complexes owes much to the study of model compounds where magnetostructural correlations can be established in a systematic way. Thus exchange-coupled polymetallic systems constitute a common ground for at least two areas of current interest, molecular magnetism and metal sites in biology. Of particular concern in this context is the development of directed routes to specific complexes, particularly those in which the metals are connected by "robust" ligands so that fragmentation of the complexes in their subsequent reactions is inhibited. One particularly successful route involves the use of "metalloligands"[10,11] in which the ligands already bound to one metal have free co-ordination sites that can bind a second metal of the same or different kind. We have previously used the same strategy utilizing "metal oximates" building blocks as ligands, to synthesize various homo- and hetero-metal complexes containing two,[12] three[13] or four[14] metal centres. Thus we have reported a series of complexes of the type M_AM_B, $M_AM_BM_A$, $M_AM_BM_BM_A$ and $(M_A)_2(\mu_3\text{-}O)_2(M_B)_2$, which have been proved to be ideal materials for the investigations of exchange mechanisms.

As an extension of the strategy of using "metal complexes" as bridging groups, we envisaged the possibility of preparing a series of linear trinuclear complexes containing three different metals $M_AM_BM_C$,[15] where two metal ions, *e.g.* M_A and M_B, are embedded in a dicompartmental imine-oxime ligand H_4LOX, synthesized by stepwise metal template condensation of the dialdehyde 2,6-diformyl-4-methylphenol and 1,3-diaminopropane, followed by oxime formation through hydroxylamine. Such a building block used in this work is shown below. Some

$Ni^{II}Cu^{II}(HLOX^{3-})$ =

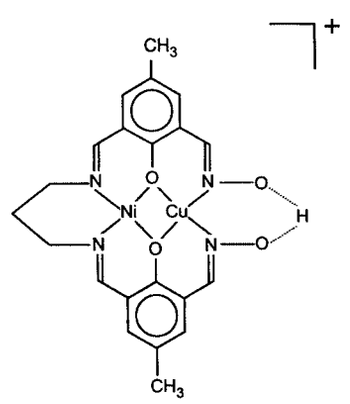

examples of dicopper complexes with this dicompartmental Schiff base oxime ligand have been reported.[16] Homodinuclear complexes of the dioxime ligand 2-hydroxy-5-methylbenzene-1,3-dicarbaldehyde dioxime[17] and heterodinuclear $Ni^{II}Cu^{II}$ complexes of some related ligands have also been described.[18–22]

The above synthetic strategy has successfully been applied to prepare several linear trinuclear heterometal complexes and in a short communication[15] we have reported the dication $[(tmtacn)Fe^{III}(Cl)Cu^{II}(CH_3OH)(LOX)Ni^{II}(CH_3OH)_2]^{2+}$ **1**, where tmtacn is the tridentate macrocyclic amine ligand 1,4,7-trimethyl-1,4,7-triazacyclononane. Complex **1** exhibits a nearly linear $Fe^{III}Cu^{II}Ni^{II}$ core in which the terminal metal centres Fe^{III}

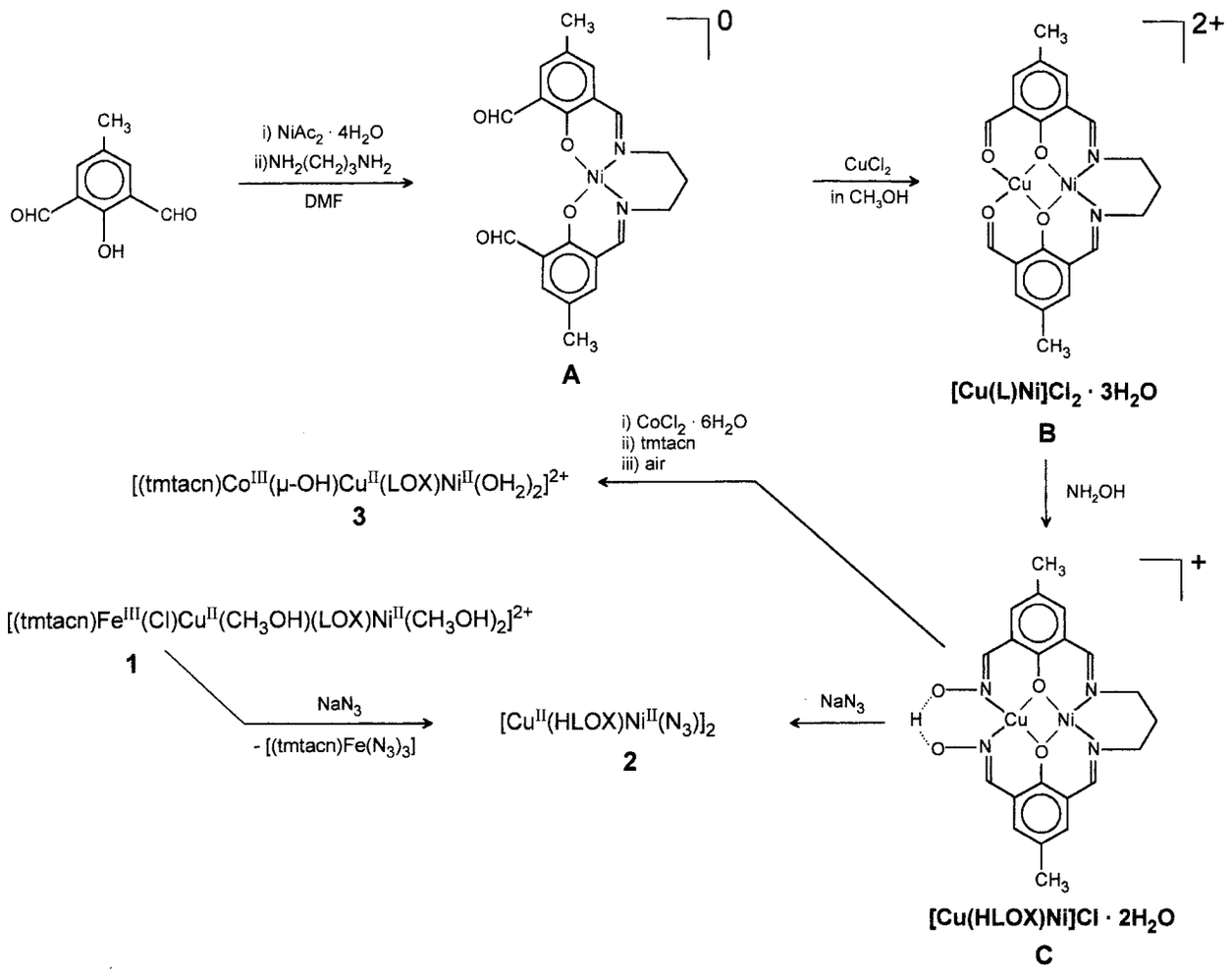

Scheme 1

and Ni^{II} adopt an octahedral co-ordination geometry, whereas the central Cu^{II} is in a square-pyramidal environment. The subject of this paper is the syntheses, structures, magnetic and spectroscopic characterization of tetranuclear $[\{Cu^{II}(HLOX)Ni^{II}(N_3)\}_2]$ **2** and trinuclear $[(tmtacn)Co^{III}(\mu\text{-}OH)Cu^{II}(LOX)Ni^{II}(OH_2)_2][ClO_4]_2$ **3**. Complex **2**, although present as a "dimer of dimer", $[Cu^{II}Ni^{II}]_2$, in the solid state, dissociates to the heterodimetallic $Cu^{II}Ni^{II}$ species in solution, as will be evident later from the EPR measurements. Complex **3** contains the same dimetallic $Cu^{II}Ni^{II}$ core as in **1** and **2**, but the capping paramagnetic (tmtacn)Fe^{III} fragment in **1** has been replaced by the diamagnetic (tmtacn)Co^{III} capping agent.

Results and discussion

A straightforward, clean and relatively high-yield synthetic route to the pure heteronuclear complex $[\{Cu^{II}(HLOX)Ni^{II}(N_3)\}_2]$ **2** is outlined in Scheme 1. More than a 5-fold excess of NH_2OH leads to the formation of intractable matter and hence was avoided. Similarly the reaction temperature was kept below 60 °C assuring the avoidance of metal scrambling. All attempts to isolate the dioxime H_2LOX were unsuccessful. The IR spectrum of **2** exhibits a strong sharp band at 2042 cm^{-1} which is assigned to the antisymmetric ν(N–N) stretching frequency of the azide groups, and a medium peak at 1314 cm^{-1} (ν_{sym}(N–N)), which has not been identified unambiguously due to overlapping bands in this region of the co-ordinated imine-oxime ligand. The strong band at 1636 cm^{-1} is unambiguously assignable to the ν(CN) vibration. The bands of medium strength at 1113, 1086 and 1069 cm^{-1} are attributed to the N–O stretching vibrations from the oxime groups.

Treatment of the heterotrinuclear complex $Fe^{III}Cu^{II}Ni^{II}$ **1** with an excess of azide results also in the formation of **2** and $[Fe^{III}(tmtacn)(N_3)_3]$ in reasonable yield (Scheme 1).

The red-brown solution obtained from cobalt(II) chloride and the macrocyclic amine in methanol–water reacting with $[Ni^{II}Cu^{II}(HLOX)]Cl$ affords upon addition of the perchlorate counter ion in the presence of air dark green crystals of **3**, containing the $Co^{III}Cu^{II}Ni^{II}$ core. The function of added triethylamine is to provide a basic medium needed for the deprotonation of the O · · · H · · · O groups present in solid $[Ni^{II}Cu^{II}(HLOX)]^+$ and for the oxidation of Co^{II} to Co^{III} by air. In the infrared spectrum of **3** a broad strong band is observed at 3407 cm^{-1} due to the ν(O–H) stretching mode. The strong band at 1081 cm^{-1} and the sharp band at 626 cm^{-1}, due to the antisymmetric stretch and antisymmetric bend of perchlorate ions, are indicative of their unco-ordinated nature. The other important strong bands are at 1636 and 1121 cm^{-1} and are assignable to ν(CN) and ν(NO) vibrations, respectively.

The optical spectra of complexes **1**, **2** and **3** have been measured in the range 200–1400 nm in dry dimethylformamide. On the basis of their high absorption coefficients and the relative sharpness, the bands can be ascribed to charge-transfer transitions within the ligands or metal-to-ligand charge transfer (MLCT). The bands at 1070, 583 nm and a shoulder at 698 nm for **2**, 983, 750 and 585 nm for **3** are thought to be due to ligand-field (d–d) transitions. For **1**, only one d-d transition at 743 nm has been observed.

Description of the structures

$Fe^{III}Cu^{II}Ni^{II}$ 1. The structure has been reported in a previous publication.[15]

Table 1 Selected bond lengths (Å) and angles (°) for [{Cu(HLOX)-Ni(N_3)}$_2$]·2CH_3OH

Cu–N(4)	1.9402(12)	Cu–N(1)	1.9504(12)
Cu–O(4)	1.9534(10)	Cu–O(3)	1.9566(10)
Ni–N(3)	2.0036(12)	Ni–N(2)	2.0012(12)
Ni–O(3)	2.0374(11)	Ni–O(4)	2.0373(10)
Ni–N(5)	2.2072(13)	Ni–O(2)	2.1814(11)
O(1)–N(1)	1.386(2)	O(2)–N(4)	1.3803(14)
N(4)–Cu–N(1)	97.28(5)	N(4)–Cu–O(4)	166.03(4)
N(1)–Cu–O(4)	91.22(4)	N(4)–Cu–O(3)	90.40(4)
N(1)–Cu–O(3)	171.60(4)	O(4)–Cu–O(3)	80.59(4)
N(2)–Ni–N(3)	99.53(5)	N(2)–Ni–O(4)	91.98(4)
N(3)–Ni–O(4)	168.18(4)	N(2)–Ni–O(3)	168.67(4)
N(3)–Ni–O(3)	91.79(4)	O(4)–Ni–O(3)	76.72(4)
N(2)–Ni–O(2)	90.67(5)	N(3)–Ni–O(2)	89.94(4)
O(4)–Ni–O(2)	92.62(4)	O(3)–Ni–O(2)	88.99(4)
N(2)–Ni–N(5)	91.85(5)	N(3)–Ni–N(5)	92.59(5)
O(4)–Ni–N(5)	84.31(4)	O(3)–Ni–N(5)	87.95(5)
O(2)–Ni–N(5)	176.09(4)	Cu–O(4)–Ni	101.25(4)
Cu–O(3)–Ni	101.14(4)		

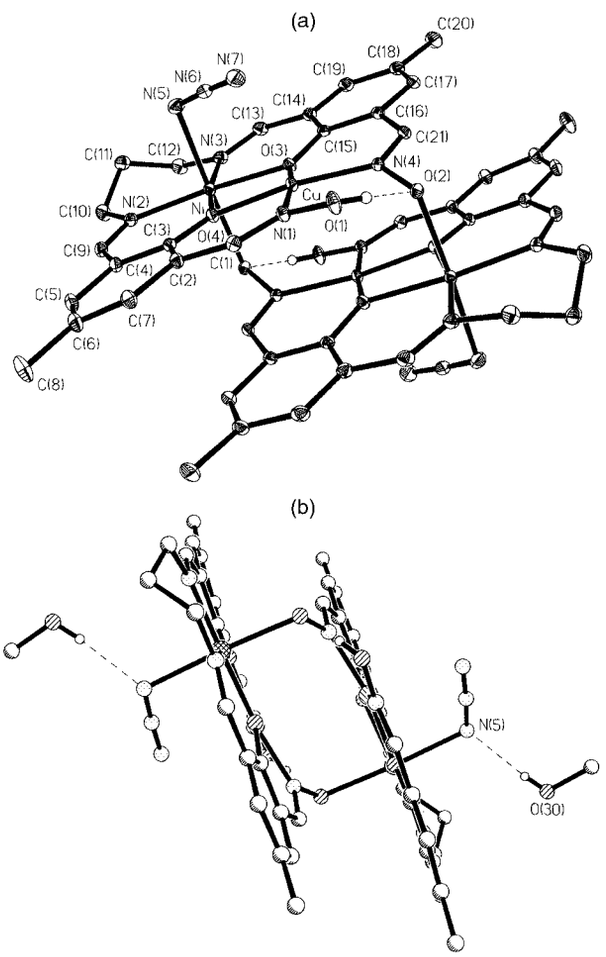

Fig. 1 (a) Molecular structure of [{Cu^{II}(HLOX)Ni^{II}(N_3)}$_2$] **2**, showing the protonated oximic oxygen. (b) A perspective view of **2** highlighting the connectivity between the two $Cu^{II}Ni^{II}$ units, together with two solvent methanol molecules.

[{Cu^{II}(HLOX)Ni^{II}(N_3)}$_2$] 2. Complex **2**, [{Cu^{II}(HLOX)Ni^{II}-(N_3)}$_2$], shows a centrosymmetric tetranuclear structure [CuNi]$_2$ (Fig. 1(a) and (b)) with both nickel(II) centres having six-co-ordinated geometries NiN_3O_3, whereas both Cu^{II} in square-planar CuN_2O_2 stereochemistries. A crystallographic centre of inversion lies at the midpoint of the Ni · · · Ni vector. Selected bond lengths and angles are listed in Table 1. The neighbouring nickel and copper ions in the ligand plane are bridged together through the phenolate oxygen atoms, O(3) and O(4). Each copper is bound to two nitrogens, N(1) and N(4), of the oxime groups, one of which is protonated at O(1) and the other deprotonated oxygen O(2) occupies the axial position of the crystallographically related second nickel by an inversion centre. The azide ions are bound only to nickel ions. In this regard **2** differs from the reported[23] [{Cu(oxpn)Ni(μ-NCS)-(OH_2)(tmen)}$_2$]$^{2+}$, in which two dinuclear [Cu(oxpn)Ni(OH_2)-(tmen)] entities [oxpn = *N*,*N*′-bis(3-aminopropyloxamide)] are linked by two Cu–SCN–Ni bridging units, related by an inversion centre. In contrast, the bis(heterodinuclear) complex **2** is built up of two heterodinuclear [Cu(HLOX)Ni(N_3)] units, which are held together by two deprotonated oxime oxygens. Each of the oxygens, O(4) and O(2), is bound respectively to an axial position of nickel ions. The bridging network NiO(3)O(4)Cu is nearly planar with NiOCu angles of 101.2° and a Cu · · · Ni separation of 3.085 Å.

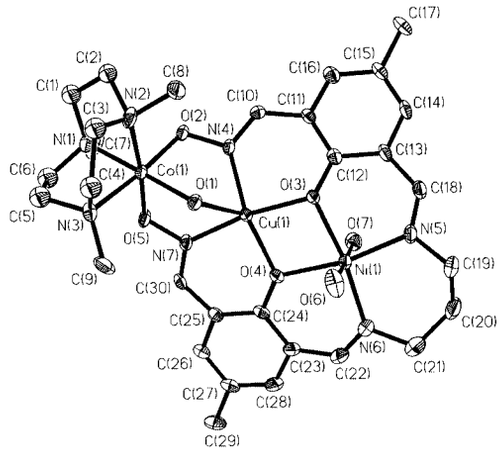

Fig. 2 Structure of the dication containing the $Co^{III}Cu^{II}Ni^{II}$ units in crystals of complex **3**.

The nickel centre is co-ordinated to two azomethine nitrogen atoms, N(2) and N(3), and two phenolate oxygen atoms O(3) and O(4) in the equatorial plane. The Ni–N (azomethine) (average 2.003(2) Å) and Ni–O (phenolate) (average 2.037(1) Å) bond lengths are very similar to those of the analogous complexes reported previously by us[14b] and others.[17a] The deviation of the nickel ion from the mean plane comprising NiN(2)-N(3)O(3)O(4) is only 0.019 Å. The dihedral angle between the nickel plane and the plane CuN(1)N(4)O(3)O(4) is 5.1°.

The copper centre adopts a square planar geometry by co-ordinating to two oxime nitrogen atoms, N(1) and N(4), with an average Cu–N bond length of 1.945(5) Å and to bridging phenolate oxygens O(3) and O(4) with an average Cu–O distance of 1.955(3) Å. These values are in good agreement with those in compounds containing the same ligand H_4LOX with cores like $Cu^{II}Cu^{II}$,[16] $Fe^{III}Cu^{II}Ni^{II}$ **1**[15] and $Co^{III}Cu^{II}Ni^{II}$ **3** and other comparable structures.[20] The copper ion is displaced by 0.115 Å from the mean basal plane comprising N(1)N(4)-O(3)O(4). The nearest Cu · · · Ni distance is 3.085 Å in the ligand plane, while the same between the ligand planes is 4.039 Å.

The N–O (average 1.383(3) Å) and C=N (average 1.286(6) Å) bond lengths and C–N–O bond angle (average 114.2(9)°) of the bridging oxime groups are found to be very similar to those of other comparable structures.[12–14]

[(tmtacn)Co^{III}(μ-OH)Cu^{II}(LOX)Ni^{II}(OH_2)$_2$][ClO_4]$_2$·CH_3OH·2H_2O 3. Fig. 2 shows the structure of the complex dication in **3** containing the trinuclear core Co^{III}(l.s.)$Cu^{II}Ni^{II}$ (l.s. = low spin). Selected bond lengths are listed in Table 2. The co-ordination geometry of the terminal cobalt, Co(1), is distorted octahedral with three nitrogen atoms, N(1), N(2) and N(3), from the facially co-ordinated macrocyclic amine, two oxygen atoms O(2) and O(5) from the oxime ligands and a bridging hydroxide ion, O(1) resulting in the *fac* CoN_3O_3 core. The average Co–O

Table 2 Selected bond lengths (Å) and angles (°) for [(tmtacn)Co(μ-OH)Cu(LOX)Ni$(OH_2)_2$][$ClO_4]_2$·CH_3OH·$2H_2O$ **3**

Ni(1)–N(5)	1.997(5)	Ni(1)–N(6)	2.002(6)
Ni(1)–O(4)	2.012(4)	Ni(1)–O(3)	2.035(4)
Ni(1)–O(6)	2.109(5)	Ni(1)–O(7)	2.113(5)
Co(1)–O(5)	1.880(4)	Co(1)–O(2)	1.886(4)
Co(1)–O(1)	1.913(4)	Co(1)–N(3)	1.992(5)
Co(1)–N(1)	1.994(5)	Co(1)–N(2)	2.003(5)
Cu(1)–N(7)	1.951(5)	Cu(1)–O(4)	1.958(4)
Cu(1)–O(3)	1.967(4)	Cu(1)–N(4)	1.969(5)
Cu(1)–O(1)	2.432(4)	N(7)–O(5)	1.366(6)
N(4)–O(2)	1.367(6)		
N(5)–Ni(1)–N(6)	97.8(2)	N(5)–Ni(1)–O(4)	168.8(2)
N(6)–Ni(1)–O(4)	93.4(2)	N(5)–Ni(1)–O(3)	91.5(2)
N(6)–Ni(1)–O(3)	170.4(2)	O(4)–Ni(1)–O(3)	77.2(2)
N(5)–Ni(1)–O(6)	91.3(2)	N(6)–Ni(1)–O(6)	89.1(2)
O(4)–Ni(1)–O(6)	89.3(2)	O(3)–Ni(1)–O(6)	93.0(2)
N(5)–Ni(1)–O(7)	89.5(2)	N(6)–Ni(1)–O(7)	91.7(2)
O(4)–Ni(1)–O(7)	89.8(2)	O(3)–Ni(1)–O(7)	86.1(2)
O(6)–Ni(1)–O(7)	178.9(2)	N(7)–Cu(1)–O(4)	90.0(2)
N(7)–Cu(1)–O(3)	169.9(2)	O(4)–Cu(1)–O(3)	80.1(2)
N(7)–Cu(1)–N(4)	99.7(2)	O(4)–Cu(1)–N(4)	164.7(2)
O(3)–Cu(1)–N(4)	89.6(2)	N(7)–Cu(1)–O(1)	76.1(2)
O(4)–Cu(1)–O(1)	118.9(2)	O(3)–Cu(1)–O(1)	110.4(2)
N(4)–Cu(1)–O(1)	75.3(2)	O(5)–Co(1)–O(2)	89.8(2)
O(5)–Co(1)–O(1)	92.2(2)	O(2)–Co(1)–O(1)	93.2(2)
O(5)–Co(1)–N(3)	91.1(2)	O(2)–Co(1)–N(3)	174.4(2)
O(1)–Co(1)–N(3)	92.2(2)	O(5)–Co(1)–N(1)	87.9(2)
O(2)–Co(1)–N(1)	88.2(2)	O(1)–Co(1)–N(1)	178.5(2)
N(3)–Co(1)–N(1)	86.3(2)	O(5)–Co(1)–N(2)	174.3(2)
O(2)–Co(1)–N(2)	92.1(2)	O(1)–Co(1)–N(2)	93.1(2)
N(3)–Co(1)–N(2)	86.5(2)	N(1)–Co(1)–N(2)	86.8(2)
Co(1)–O(1)–Cu(1)	98.1(2)		
Cu(1)–O(3)–Ni(1)	100.6(2)		
Cu(1)–O(4)–Ni(1)	101.8(2)		

and Co–N distances at 1.996(5) and 1.893(18) Å, respectively, are consistent with a d^6 low-spin electron configuration of the cobalt centre.[24] The Co–Cu–Ni skeleton is not linear with an angle of 155.6°, whereas the angle Fe–Cu–Ni in **1** is 174°.[15] The intramolecular separations between the metal centres Co · · · Cu 3.299, Cu · · · Ni 3.081 and Co · · · Ni 6.236 Å are in conformity with the values observed earlier for comparable structures.[15] The dihedral angle between the basal copper plane Cu(1)N(4)-N(7)O(3)O(4) and the equatorial Ni plane Ni(1)N(5)N(6)-O(4)O(3) is 175.4°. The corresponding dihedral angle in **1** is very similar, 169.4°. Accordingly, the Cu · · · Ni separations in **1** and **3** are not different; Cu · · · Ni in **1** 3.087 Å.[15]

The geometry of the central coper(II) centre is distorted square pyramidal, with the elongated fifth bond (2.432 Å) to axially co-ordinated oxygen atom O(1) of the μ-OH ligand. The angles O(1)Cu(1)N(7) and O(1)Cu(1)N(4) are noticeably less (76.1 and 75.3°) than 90°, thus making the CoN_3O_3 octahedron tipped toward the equatorial copper plane Cu(1)N(4)N(7)-O(4)O(3). Accordingly, the Co–Cu–Ni skeleton in **3** is not linear in contrast to the Fe–Cu–Ni skeleton of **1**. The metrical parameters for the copper centre are very similar to those of the copper dimer with the same Schiff-base oxime ligand.[16]

The terminal nickel ion, Ni(1), is co-ordinated equatorially to the azomethine nitrogen atoms, N(5) and N(6), and two bridging phenolate groups, O(3) and O(4), from the Schiff base oxime ligand. The nickel centre adopts a six-co-ordinated environment by interacting with two *trans* axially disposed water molecules, O(6) and O(7). The nickel centre is displaced by 0.022 Å from the mean basal plane comprising O(3)O(4)-N(5)N(6). The equatorial Ni–N and Ni–O (phenolate) distances are nearly equal, average 2.000(6) and 2.024(12) Å, respectively. The Ni–OH_2 distances are rather long, average 2.111(5) Å, as has been observed earlier.[17a,25] The bridging angles Cu(1)–O(3)–Ni(1) and Cu(1)–O(4)–Ni(1) are nearly equal 100.6(2) and 101.8(2)°, respectively. Thus the CuNi centres embedded in the Schiff base oxime ligand can be described as edge sharing between a square pyramid and an octahedron.

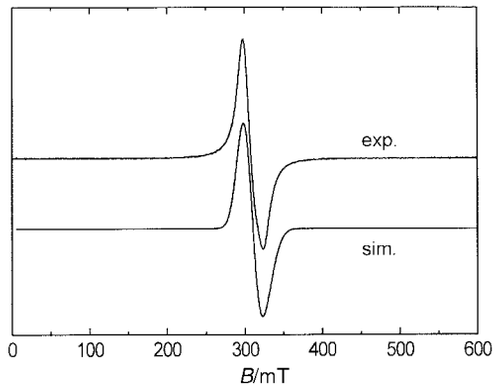

Fig. 3 Simulated and experimental X-band EPR spectra for a solid sample of complex **2** at 10 K (microwave frequency 9.650 GHz; power 100 μW; modulation amplitude 11.43 G).

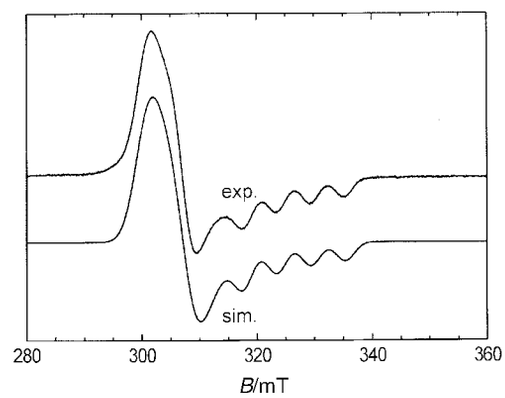

Fig. 4 X-Band EPR spectrum of complex **2** in DMF at 10 K (microwave frequency 9.644 GHz; power 100 μW; modulation amplitude 11.43 G) together with the simulated spectrum.

EPR spectroscopy

Complex **2**, [{Cu^{II}(HLOX)$Ni^{II}(N_3)$}$_2$], both as a solid and in frozen DMF solution was subjected to EPR spectroscopy and the spectra are shown in Figs. 3 and 4. Fig. 3 was obtained for a powdered sample of **2** at 10 K and X-band frequency. A broad single line emerges which can be simulated with parameters given below. In DMF glass at 10 K the spectral resolution is considerably enhanced. The EPR spectrum (Fig. 4) is of axial pattern with slightly rhombic distortion with $g_\perp$ seen at ≈2.26 together with a $g_\parallel \approx 2.1$ signal split by four copper hyperfine lines. Both solid and solution spectra were simulated with $g_x = 2.285$, $g_y = 2.239$, $g_z = 2.111$, $A_x = A_y = 7 \times 10^{-4}$ cm^{-1} and $A_z = 58 \times 10^{-4}$ cm^{-1}. The presence of hyperfine structure only in the solution spectrum strongly suggests decomposition of the tetranuclear species (dimer of dimer) into two dinuclear units in the presence of a strongly co-ordinating solvent like DMF.

It is noteworthy that the relation $g_\parallel > g_\perp$ is typical of axially symmetric d^9 Cu^{II}($S_{Cu} = \frac{1}{2}$) having one unpaired electron in a $d_{x^2-y^2}$ orbital[26] whereas $g_\parallel < g_\perp$ is observed for Cu^{II} with the unpaired electron in a d_{z^2} orbital. Axially symmetric **2** in solution exhibits features of $S = \frac{1}{2}$ with *inverted g* values ($g_\parallel < g_\perp$), keeping in mind in this regard that we are observing the doublet ground state ($S_t = \frac{1}{2}$) arising from the antiferromagnetic exchange coupling between $S_{Cu} = \frac{1}{2}$ and $S_{Ni} = 1$ in a $Cu^{II}Ni^{II}$-containing dinuclear unit. The molecular g_z axis of **2**, defined as the Cu · · · Ni axis in an idealized O_h symmetry, is perpendicular to the local g_z axis of the Cu^{II}, thus causing the inversion of the observed *g* values, *i.e.*, four unequally spaced intense features in the high-field region. The four hyperfine lines in spin-coupled $Cu^{II}Ni^{II}$ are easy to understand, as only Cu has isotopes ^{63}Cu

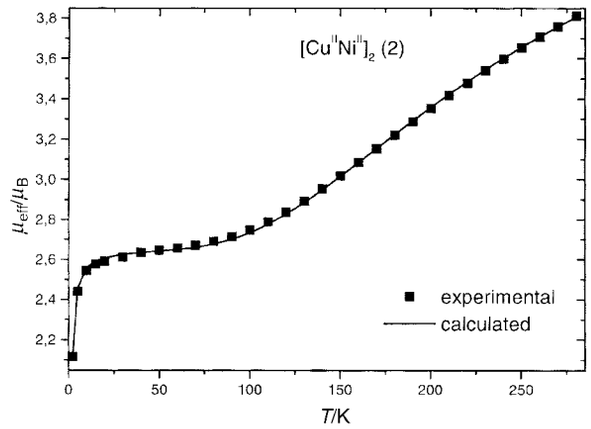

Fig. 5 Temperature dependence of the magnetic moments for complex **2**. The solid line represents the best least-squares fit of the experimental data by the Heisenberg–Dirac–Van Vleck model.

(69.1%) and ^{65}Cu (30.9%) with $I_{Cu} = \frac{3}{2}$, whereas Ni has isotope ^{61}Ni with $I_{Ni} = \frac{3}{2}$, but its natural abundance is very low, 1.25%. Thus the hyperfine structure due to only the copper nucleus is observed for exchange-coupled $Cu^{II}Ni^{II}$. For the spin-doublet ground state of **2** in solution the hyperfine coupling constant A'_{Cu} is related to the hyperfine coupling constant A_{Cu} for a mononuclear copper(II) complex by the expression $A'_{Cu} = -A_{Cu}/3$. The hyperfine coupling constant $A_z = 58 \times 10^{-4}$ cm^{-1} evaluated for **2**, which is indeed one-third of the A_{Cu} range observed generally for mononuclear d^9 copper(II) systems,[27] confirms therefore the binuclear nature of **2** in solution. The EPR spectrum of **2** exhibiting copper hyperfine structure in the high field regions clearly indicates that the unpaired electron in the ground state for **2** resides on the molecular orbital of d_{z^2} character comprising d_z^2(Cu) and d_z^2(Ni) and is delocalized over the CuNi core.

The $Co^{III}Cu^{II}Ni^{II}$ complex, **3**, in water–CH_3OH glass exhibits an EPR spectrum at 10 K which is nearly identical with that of **2** in solution. Like **2**, this signal can be assigned to a transition $|\frac{1}{2}, -\frac{1}{2}\rangle \longrightarrow |\frac{1}{2}, \frac{1}{2}\rangle$ of the $S_t = \frac{1}{2}$ ground state for **3**. The simulated parameters for **3** are $g_1 = 2.273$, $g_2 = 2.236$, $g_3 = 2.099$ and a clear four-line hyperfine structure with $A_3 = 54 \times 10^{-4}$ cm^{-1} and $A_\perp \leq 2 \times 10^{-4}$ cm^{-1} is superposed on the g_3 component due to the copper nucleus, thus strongly favouring the d_{z^2} character of the molecular orbital of the $S_t = \frac{1}{2}$ ground state for **3**.

Magnetic susceptibility studies

Magnetic susceptibility data (SQUID) for polycrystalline samples of complexes **2** and **3** were collected over the temperature range 2–290 K. Fig. 5 shows the variable-temperature magnetic susceptibility for **2** in the form of a μ_{eff} *vs.* T plot. At 290 K the μ_{eff} value of 3.86 μ_B ($\chi_m T = 1.873$ cm^3 mol^{-1} K) is considerably lower than that of 4.69 μ_B expected for a compound containing two $S = \frac{1}{2}$ (Cu^{II}) and two $S = 1$ (Ni^{II}) uncoupled spins. When the complex is cooled to about 60 K, μ_{eff} decreases monotonically reaching a plateau defined by $\mu_{eff} = 2.66$ μ_B ($\chi_m T = 0.888$ cm^3 mol^{-1} K). Below 40 K the magnetic moment decreases very slowly to a value of 2.54 μ_B ($\chi_m T = 0.813$ cm^3 mol^{-1} K) at 10 K and then starts to decrease rapidly reaching a value of 2.12 μ_B ($\chi_m T = 0.564$ cm^3 mol^{-1} K) at 2 K. This magnetic behaviour is completely in accord with antiferromagnetically interacting spins of $S = 1$ and $\frac{1}{2}$, leading to a spin-doublet ($^2A_1$ in C_{2v} symmetry) ground state. Below 60 K the excited quartet $^4A_1$ state is totally depopulated.

We applied the usual Heisenberg–Dirac–van Vleck (HDvV) exchange Hamiltonian in the form (1) with $S_{Ni(1)} = S_{Ni(2)} = 1$ and

$$\hat{H} = -2J(S_{Ni(1)} \cdot S_{Cu(1)} + S_{Ni(2)} \cdot S_{Cu(2)}) - 2J'(S_{Ni(1)} \cdot S_{Cu(2)} + S_{Ni(2)} \cdot S_{Cu(1)}) \quad (1)$$

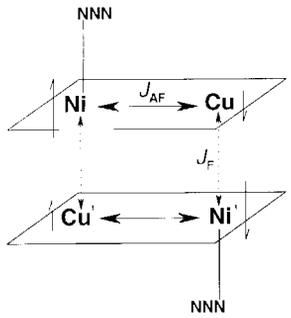

Fig. 6 Schematic representation of the interactions J_{AF} and J_F between the two hetero-dimeric units $Cu^{II}Ni^{II}$ in complex **2**.

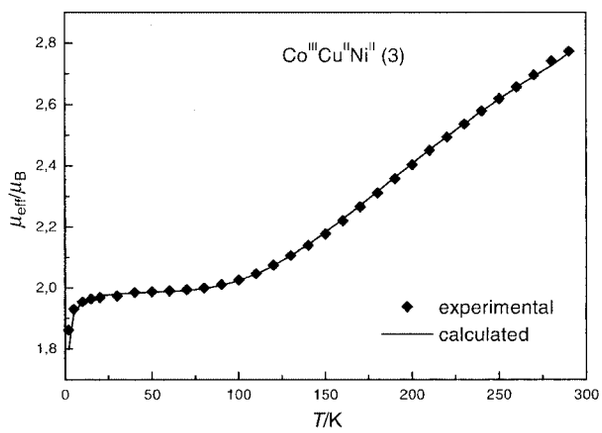

Fig. 7 Effective magnetic moment as a function of temperature for complex **3**. The solid line represents the simulation with the spin Hamiltonian (see text).

$S_{Cu(1)} = S_{Cu(2)} = \frac{1}{2}$, where J corresponds to the coupling between neighbouring Ni^{II} and Cu^{II} through the phenolate bridges (*intra*-dimer) and J' to the coupling through the oximato bridges (*inter*-dimer). The experimental magnetic data were simulated using a least-squares fitting computer program[28] with a full-matrix diagonalization approach including exchange coupling, Zeeman splitting and zero-field interactions (DS^2_z), if necessary. The best fit shown as the solid line in Fig. 5 results in $J = -114.9$ cm^{-1}, $J' = +0.96$ cm^{-1}, $g_{Ni} = 2.16$ (fixed), $g_{Cu} = 2.12$ (fixed), $D = 0$ (fixed) and temperature independent paramagnetism (TIP) = 134×10^{-6} cm^3 mol^{-1}. These data correspond to a strong antiferromagnetic coupling, J, between the neighbouring Cu^{II}/Ni^{II} centres (*intra*-dimer) as well as a weak ferromagnetic coupling, J', between the Cu^{II}/Ni^{II} pairs through the oximato bridges. We have found that the experimental data could not be fitted with only J; J' is absolutely necessary to fit the data satisfactorily. Additionally, as a variation of D between 0 and 10 cm^{-1} has no influence on the quality of the fitting, we have kept $D = 0$ (fixed) during the simulation. The spin interactions, J and J', for complex **2** are shown schematically as J_{AF} and J_F in Fig. 6. It is interesting that a ferromagnetic coupling through oximato bridges is not very common.[29] Indeed, bridging oximate groups are known to be very efficient in mediating very strong antiferromagnetic interactions, which are provided by an orbital exchange pathway essentially of σ nature.[12,13] As the doublet–quartet $^2A_1 \leftrightarrow {}^4A_1$ separation is large (345 cm^{-1}) for **2**, the influence of the zero-field splitting on the magnetic behaviour of **2** is negligible, justifying $D = 0$ kept fixed during the simulation.

The cryomagnetic property of complex **3** is shown in Fig. 7 in the form of a μ_{eff} *vs.* T plot. The magnetic moment of 2.85 μ_B ($\chi_m T = 1.017$ cm^3 mol^{-1} K) at 290 K decreases steadily with decreasing temperature, reaching a value of 2.03 μ_B ($\chi_m T = 0.5145$ cm^3 mol^{-1} K) at 80 K which remains nearly constant until 15 K with a value of 1.97 μ_B ($\chi_m T = 0.4833$ cm^3 mol^{-1} K) and then starts to decrease reaching a value of 1.86 μ_B

Table 3 Selected magnetic and structural parameters for doubly phenoxide-bridged heterodinuclear $Cu^{II}Ni^{II}$ complexes ($H = -2JS_1 \cdot S_2$)

Compound[a]	Cu ··· Ni/Å	J/cm^{-1}	Cu–O–Ni/°	Ref.
[Ni((prp)$_2$en)Cu(hfa)$_2$]	≈3.0	−48	100.8	18
[CuNi((fsa)$_2$en)(OH$_2$)$_2$]·H$_2$O	2.975	−71	98.9	20
[{Cu(salen)Ni(hfa)$_2$}$_2$]	2.897	−11.8	93.9	21
[CuNiL][ClO$_4$]$_2$·H$_2$O·2DMF	3.038	−90	99.9	22
1 $Fe^{III}Cu^{II}Ni^{II}$	3.087	−118.6	101.6	15
2 $Cu^{II}Ni^{II}$	3.085	−115	101.1	This work
3 $Co^{III}Cu^{II}Ni^{II}$	3.081	−130	100.7	This work, 15

[a] (prp)$_2$en = *N*,*N*′-ethylenebis(2-hydroxypropiophenone iminato)(2−); hfa = hexafluoroacetylacetonate; H$_4$(fsa)$_2$en = *N*,*N*′-bis(3-carboxy-2-hydroxybenzylidene)-1,2-diaminoethane, H$_2$salen = *N*,*N*′-bis(salicylidene)-1,2-diaminoethane; H$_2$L = a dinucleating macrocycle derived from the [2:1:1] condensation of 2,6-diformyl-4-methylphenol, 1,2-diaminoethane and 1,4-diaminobutane.

($\chi_m T = 0.4321$ cm^3 mol^{-1} K) at 2 K. This magnetic behaviour is quite characteristic of antiferromagnetic coupling between the paramagnetic nickel(II) and copper(II) centres. The least-squares fitting, shown as the solid line in Fig. 7, of the experimental data leads to $J = -130$ cm^{-1}, $g_{Cu} = 2.24$ (fixed) and $g_{Ni} = 2.27$ (fixed). A temperature-independent paramagnetism of 360×10^{-6} cm^3 mol^{-1} was also considered to achieve the excellent fit shown in Fig. 7. Thus the copper and nickel centres in **3** are antiferromagnetically exchange coupled with a doublet ground state, and the excited quartet state lying 375 cm^{-1} above the ground state. Thus, as is expected, the low-lying electronic states for **2** and **3** are nearly identical.

The relatively small linewidth and the lack of hyperfine splitting by the ^{59}Co ($I = \frac{7}{2}$) nucleus in the EPR spectrum of complex **3** at 10 K are clear indications that **3** is a Co^{III}-$Cu^{II}Ni^{II}$ species with localized Co^{III}($S_{Co} = 0$), Cu^{II}($S_{Cu} = \frac{1}{2}$), Ni^{II}($S_{Ni} = 1$) oxidation states.

Spin multiplets in the complexes **2** and **3** are well separated by exchange interactions. Under this condition, the g values of the different spin multiplets can be related to local values of individual metal ions with spin-dependent weight factors derived from the Wigner–Eckart theorem.[30,31] The g values for the spin states $S_t = \frac{1}{2}$ and $\frac{3}{2}$ of **2** and **3** are related to those of the local copper and nickel ions by eqns. (2) and (3). The ground-state

$$g_{3/2} = (\tfrac{1}{3}g_{Cu} + \tfrac{2}{3}g_{Ni}) \quad (2)$$

$$g_{1/2} = (-\tfrac{1}{3}g_{Cu} + \tfrac{4}{3}g_{Ni}) \quad (3)$$

properties of **2** and **3** are dominated by Ni^{II} as is shown clearly by the relation for $g_{1/2}$ given above. Using the simulated g_{Cu} and g_{Ni} values from the susceptibility data of **3** in the above relation for $g_{1/2}$, one obtains $g_{1/2}$ of 2.280 which deviates appreciably from the g_{av} of 2.203 obtained from the simulation of the EPR spectrum at 10 K. On the contrary $g_{1/2}$ of 2.212 from the EPR for **2** is not far from that of 2.17 obtained from susceptibility measurements on **2**.

The mechanism of the leading phenomenon of isotropic exchange for the $Cu^{II}Ni^{II}$ pairs is now well understood.[4,20] The net exchange is composed of two competing individual antiferro- and ferro-magnetic exchange, $J[d_{x^2-y^2}(Cu) \leftrightarrow d_{x^2-y^2}(Ni)]$ and $J[d_{x^2-y^2}(Cu) \leftrightarrow d_{z^2}(Ni)]$. The dominant pathway $d_{x^2-y^2}/d_{x^2-y^2}$ is antiferromagnetic, while the pathway $d_{x^2-y^2}/d_{z^2}$ involving orthogonal magnetic orbitals is weak ferromagnetic, thus resulting in a significant overall antiferromagnetic interaction for all reported $Cu^{II}Ni^{II}$ complexes.

In the case of binuclear copper(II)[32] and nickel(II)[33] complexes linked through two phenoxide bridges, the net J is found empirically to depend on the bridging angle θ. It has been pointed out recently[17a] that these empirical relations should be treated with caution. There is far less work published on heterodinuclear $Cu^{II}Ni^{II}$ complexes and no such empirical relation between J and θ can be drawn up, as is evident from Table 3.

It is noteworthy that although the structures of complexes **2** and **3** are very similar, the strength of spin coupling in **3** is stronger than that in **2**. These results together with the compounds in Table 3 emphasize the necessity for a more intricate explanation for a complete rationalization of superexchange through two phenoxide bridges, not only for the homometallic but also for the heterometallic systems.

Experimental

Chemicals

Reagent or analytical grade materials were obtained from commercial suppliers and used without further purification. The macrocycle 1,4,7-trimethyl-1,4,7-triazacyclononane (L = $C_9H_{21}N_3$) was prepared as described previously.[34]

Physical measurements

Fourier transform infrared spectroscopy on KBr pellets was performed on a Perkin-Elmer 1720X FT-IR instrument. Electronic absorption spectra of solution were measured on a Perkin-Elmer Lambda 19 spectrophotometer (range: 220–1400 nm). Temperature-dependent (2–298 K) magnetization data were recorded on a SQUID magnetometer (MPMS, Quantum Design) in a field of 1 T. The experimental susceptibility data were corrected for underlying diamagnetism using tabulated Pascal's constants. The X-band EPR spectra of the polycrystalline material either as solid or in solution were recorded at various temperatures between 3 and 100 K with a Bruker ESP 300 spectrometer equipped with a standard TE 102 cavity, an Oxford Instruments liquid helium continuous-flow cryostat, an NMR gaussmeter, and a frequency meter.

Preparation of the compounds

2,6-Diformyl-4-methylphenol.[35] The dialdehyde, described earlier,[36] was prepared by a completely different way. To a solution of *p*-cresol (10.8 g; 0.1 mol) in acetic acid (50 cm^3) were added hexamethylenetetraamine (28.2 g; 0.2 mol) and paraformaldehyde (30 g; 1.0 mol). The system was stirred until a light brown viscous solution was formed and then heated (70–90 °C) for 2 h. The solution was cooled to room temperature and conc. H_2SO_4 (10 cm^3) carefully added. The resulting solution was refluxed again for 0.5 h and then on treatment with distilled water (400 cm^3) resulted in the formation of a light yellow precipitate, which was stored at 4 °C overnight. The yellow product was isolated by filtration and washed with a small amount of cold CH_3OH. A more pure product was obtained by means of recrystallization from toluene. Yield: 5.7 g (35%), mp 130–134 °C (lit., 133.5 °C). EI mass spectrum: *m*/*z* 164 (73.3), 136 (100%), calc. for $[C_9H_8O_3]^+$ 164. ^{1}H NMR [250.13 MHz, $CDCl_3$, 300 K]: δ 2.36 [s, 3 H (CH_3)], 7.75 [s, 2 H (aryl H)], 10.19 [s, 2 H (CHO)] and 11.43 [s, 1 H (OH)]. IR(KBr, cm^{-1}): 1682s, 1666vs, 1216m and 2871w.

[Ni(L)] A (Scheme 1). To a solution of 2,6-diformyl-4-methylphenol (3.0 g; 18 mmol) in warm dry dimethylformamide

(40 cm^3) under constant stirring was added dropwise 1,3-diaminopropane (81.13 g; 15 mmol). Solid $NiAc_2·4H_2O$ (2.3 g; 9 mmol) was added and the solution was kept at 50 °C for 1 h when a brown-yellow solid precipitated; the solid was warm-filtered and washed with i-PrOH and diethyl ether. Yield: 1.74 g (45%).

[Cu(L)Ni]Cl_2·3H_2O B (Scheme 1). To a vigorously stirred suspension of complex A (0.84 g; 2.0 mmol) in methanol (20 cm^3) a methanolic solution (10 cm^3) of $CuCl_2·2H_2O$ (0.34 g; 2 mmol) was added dropwise and slowly. Within 20 min the solution started to become turbid, when it was cooled at 4 °C. Addition of diethyl ether initiated precipitation of a greenish yellow powder, which was isolated by filtration and washed thoroughly with water, i-PrOH and ether. Yield: 0.96 g (79%). Calc. for $C_{21}H_{26}Cl_2CuN_2NiO_7$: C, 41.24; H, 4.28; Cu, 10.39; N, 4.58; Ni, 9.60. Found: C, 41.5; H, 4.5; Cu, 10.2; N, 4.7; Ni, 9.7%. IR(KBr, cm^{-1}): 3373m (br); 1638s, str.; 1553s, str.; 1409ms; 1340ms (s = sharp, str = strong).

[Cu(HLOX)Ni]Cl·2H_2O C (Scheme 1). Compound B (0.61 g; 1 mmol) dissolved in methanol (30 cm^3) was treated with a methanolic solution (10 cm^3) of $NH_2OH·HCl$ (0.21 g; 3 mmol) and Et_3N (0.4 g; 4 mmol) and heated at 60 °C for 1 h with continuous stirring. A green-brown solid precipitated and was collected after filtration and washing with methanol and ether. Yield: 0.43 g (73%). Calc. for $C_{21}H_{26}ClCuN_4NiO$: C, 42.96; H, 4.29; Cu, 10.83; N, 9.54; Ni, 10.0. Found: C, 43.1; H, 4.4; Cu, 10.9; N, 9.4; Ni, 9.7%. IR(KBr, cm^{-1}): 3423m (br); 1628s, str.; 1560s, str.; 1450s, str.; 1316ms.

[{Cu(HLOX)Ni(N_3)}$_2$]·2CH_3OH 2. A solid sample of NaN_3 (0.13 g; 2 mmol) was added to a warm solution of compound C (0.587 g; 1 mmol) in methanol (30 cm^3) at 60 °C with stirring. The solution was kept at 60 °C for 0.5 h without stirring, when crystallization started. The green crystals were collected by filtration and air-dried. Yield: 0.95 g (80%). Calc. for $C_{22}H_{25}CuN_7NiO_5$: C, 44.81; H, 4.27; Cu, 10.78; N, 16.63; Ni, 9.95. Found: C, 44.6; H, 4.3; Cu, 10.8; N, 16.5; Ni, 9.8%. IR(KBr, cm^{-1}): 2042s, str.; 1636s, str.; 1557ms; 1453ms; 1314ms; 1113, 1086 and 1069ms. UV-vis in DMF: λ/nm (ε/M^{-1} cm^{-1}) 372(25200), 583(249), 698 (sh)(≈190) and 1070(41).

[(tmtacn)Co(μ-OH)Cu(LOX)Ni(OH_2)$_2$][ClO_4]$_2$·CH_3OH·2H_2O 3. A solid sample of compound C (0.29 g; 0.5 mmol) was added in small portions to a solution of 1,4,7-trimethyl-1,4,7-triazacyclononane (0.085 g; 0.5 mmol) in water–methanol (15 : 30 cm^3) containing $CoCl_2·6H_2O$ (0.13 g; 0.5 mmol). After addition of a small portion of Et_3N (0.5 cm^3) the resulting solution was warmed at 70 °C on a water-bath for 1 h. The solution kept at ambient temperature after addition of $NaClO_4·H_2O$ yielded green crystals. Yield: 0.28 g (53%). Calc. for $C_{31}H_{54}Cl_2CoCuN_7NiO_{18}$: C, 34.97; H, 5.11, Co, 5.53; Cu, 5.97; N, 9.21; Ni, 5.51. Found: C, 34.8; H, 5.10; Co, 5.7; Cu, 6.0; N, 9.4; Ni, 5.7%. IR(KBr, cm^{-1}): 3407 (br), str.; 1636s, str.; 1556ms; 1448ms; 1308ms; 1144ms; 1121s, str.; 1081s, vs; 626ms. UV-vis in DMF: λ/nm (ε/M^{-1} cm^{-1}): 379(16510), 585(429), 750(87) and 983(42).

X-Ray crystallography

The crystallographic data of $[Cu^{II}Ni^{II}]_2$ **2** and $Co^{III}Cu^{II}Ni^{II}$ **3** are summarized in Table 4. Graphite monochromated Mo-Kα X-radiation (λ = 0.71073 Å) was used throughout. Intensity data were corrected for Lorentz-polarization and absorption effects using the program SADABS.[37] The structures were solved by direct methods by using SHELXTL PLUS.[38] The function minimized during full-matrix least-squares refinement was $\Sigma w(|F_o| - |F_c|)^2$. Hydrogen atoms attached to carbon were placed at calculated positions and refined as riding atoms with isotropic thermal parameters. The oximic hydrogen OH was located from Fourier-difference maps and refined with restrained distances. All non-hydrogen atoms were refined with anisotropic thermal parameters.

Table 4 Crystallographic data for [{Cu(HLOX)Ni(N_3)}$_2$]·2CH_3OH **2** and [(tmtacn)Co(μ-OH)Cu(LOX)Ni(OH_2)$_2$][ClO_2]$_2$·CH_3OH·2H_2O **3**

	2	**3**
Formula	$C_{44}H_{50}Cu_2N_{14}Ni_2O_{10}$	$C_{31}H_{54}Cl_2CoCuN_7Ni$
M	1179.48	1064.88
Crystal size/mm	0.53 × 0.46 × 0.35	0.70 × 0.25 × 0.14
Crystal system	Monoclinic	Triclinic
Space group	$P2_1/n$	$P\bar{1}$
a/Å	8.726(1)	7.443(1)
b/Å	15.024(3)	14.281(2)
c/Å	17.649(3)	21.582(3)
α/°		104.04(2)
β/°	100.18(3)	96.90(2)
γ/°		104.31(2)
V/Å^3	2277.3(7)	2116.5(5)
Z	2	2
μ/mm^{-1}	1.812	1.532
No. independent reflections ($F > 4.0\sigma(F)$)	7860	7050
Data/restraints/parameters	7669/0/335	6705/0/560
$R_F(F > 4\sigma(F))$, $wR2$	0.0275, 0.0698	0.0623, 0.1635
T/K	100	293

Some parts of the structure of complex **3** were found to be disordered. The disorder of the carbon atoms of the tmtacn backbone was successfully modelled by a split atom model to yield the δδδ and λλλ form of the macrocycle. The carbon atoms were isotropically refined with occupancy factors of 0.5 for each set. Hydrogen atoms were geometrically attached to both parts and refined as riding atoms.

One of the two perchlorate anions is also disordered over two sites. Splitting of the chlorine and one oxygen atom with a ratio of 0.75 : 0.25 gave a satisfactory model of two face sharing tetrahedral parts of the anion. The mean component was anisotropically refined while the minor positions (Cl(1X) and O(10X)) were treated isotropically.

The disorder of the solvent molecules is less well understood. Cations of complex **3** are hydrogen bridged by two water molecules (O(40), O(50)) which were anisotropically refined with occupancies of 1 and 0.75, respectively. Since the crystals were grown from a water–methanol mixture residual electron density in potential solvent areas suggested two more positions of methanol molecules. An occupancy factor of 0.25 was used for methanol O(51)–C(51) near water molecule O(50) and 0.5 was given to O(60)–C(60).

CCDC reference number 186/1763.

See http://www.rsc.org/suppdata/dt/a9/a908426f/ for crystallographic files in .cif format.

Acknowledgements

We thank Deutsche Akademischer Austauschdienst for a stipend (to C. N. V.), the Fonds der Chemischen Industrie and Max-Planck-Society for support.

References

1 E. Sinn, *Coord. Chem. Rev.*, 1970, **5**, 313.
2 *Magneto-Structural Correlations in Exchange Coupled Systems*, eds. R. D. Willett, D. Gatteschi and O. Kahn, Kluwer Academic Publishers, Dordrecht, 1985.
3 *Magnetic Molecular Materials*, eds. D. Gatteschi, O. Kahn, J. S. Miller and F. Palacio, Kluwer Academic Publishers, Dordrecht, 1991.
4 O. Kahn, *Molecular Magnetism*, VCH Verlagsgesellschaft, Weinheim, 1993.

5 O. Kahn, *Adv. Inorg. Chem.*, 1995, **43**, 179.
6 K. S. Murray, *Adv. Inorg. Chem.*, 1995, **43**, 261.
7 *Research Frontiers in Magnetochemistry*, ed. C. J. O'Connor, World Scientific, Singapore, 1993.
8 See for example: R. H. Holm and E. I. Solomon (Guest Editors), *Chem. Rev.*, 1996, **96**, No. 7; A. L. Feig and S. J. Lippard, *Chem. Rev.*, 1994, **94**, 759; L. Que and A. E. True, *Prog. Inorg. Chem.*, 1990, **38**, 98.
9 S. J. Lippard and J. M. Berg, *Principles of Bioinorganic Chemistry*, University Science Books, Mill Valley, CF, 1994; W. Kaim and B. Schwederski, *Bioanorganische Chemie*, B. G. Teubner, Stuttgart, 1991; *Bioinorganic Chemistry of Copper*, eds. K. D. Karlin and Z. Tyeklár, Chapman & Hall, New York, 1993; *Mechanistic Bioinorganic Chemistry*, eds. H. Holden Thorp and V. L. Pecoraro, American Chemical Society, Washington, 1995.
10 S. J. Gruber, C. M. Harris and E. Sinn, *J. Inorg. Nucl. Chem.*, 1968, **30**, 1805; J. Selbin and L. Ganguly, *J. Inorg. Nucl. Chem. Lett.*, 1969, **5**, 815; R. L. Linkvedt, L. S. Kramer, G. Ranger, P. W. Corfield and M. D. Glick, *Inorg. Chem.*, 1983, **22**, 3580.
11 D. Luneau, H. Oshio, H. Okawa and S. Kida, *J. Chem. Soc.*, *Dalton Trans.*, 1990, 2283; S. Pal, R. Mukherjee, M. Tomas, L. R. Falvello and A. Chakravorty, *Inorg. Chem.*, 1986, **25**, 200; E. Colacio, J. M. Dominguez-Vera, A. Escuer, R. Kivekäs and A. Romerosa, *Inorg. Chem.*, 1994, **33**, 3914.
12 P. Chaudhuri, M. Winter, U. Flörke and H.-J. Haupt, *Inorg. Chim. Acta*, 1995, **232**, 125; F. Birkelbach, M. Winter, U. Flörke, H.-J. Haupt, C. Butzlaff, M. Lengen, E. Bill, A. X. Trautwein, K. Wieghardt and P. Chaudhuri, *Inorg. Chem.*, 1994, **33**, 3990; D. Burdinski, F. Birkelbach, M. Gerdan, A. X. Trautwein, K. Wieghardt and P. Chaudhuri, *J. Chem. Soc.*, *Chem. Commun.*, 1995, 963.
13 P. Chaudhuri, M. Winter, B. P. C. Della Vedova, E. Bill, A. X. Trautwein, S. Gehring, P. Fleischhauer, B. Nuber and J. Weiss, *Inorg. Chem.*, 1991, **30**, 2148; D. Burdinski, F. Birkelbach, T. Weyhermüller, U. Flörke, H.-J. Haupt, M. Lengen, A. X. Trautwein, E. Bill, K. Wieghardt and P. Chaudhuri, *Inorg. Chem.*, 1998, **37**, 1009; F. Birkelbach, U. Flörke, H.-J. Haupt, C. Butzlaff, A. X. Trautwein, K. Wieghardt and P. Chaudhuri, *Inorg. Chem.*, 1998, **37**, 2000 and references therein.
14 (*a*) P. Chaudhuri, F. Birkelbach, M. Winter, V. Staemmler, P. Fleischhauer, W. Haase, U. Flörke and H.-J. Haupt, *J. Chem. Soc.*, *Dalton Trans.*, 1994, 2313; (*b*) C. Krebs, M. Winter, T. Weyhermüller, E. Bill, K. Wieghardt and P. Chaudhuri, *J. Chem. Soc.*, *Chem. Commun.*, 1995, 1913 and references therein.
15 C. N. Verani, T. Weyhermüller, E. Rentschler, E. Bill and P. Chaudhuri, *Chem. Commun.*, 1998, 2475.
16 E. V. Rybak-Akimova, D. H. Busch, P. K. Kahol, N. Pinto, N. W. Alcock and H. J. Clase, *Inorg. Chem.*, 1997, **36**, 510.
17 (*a*) D. Black, A. J. Blake, K. P. Dancey, A. Harrison, M. McPartlin, S. Parsons, P. A. Tasker, G. Whittaker and M. Schröder, *J. Chem. Soc.*, *Dalton Trans.*, 1998, 3953; (*b*) K. K. Nanda, A. W. Addison, N. Paterson, E. Sinn, L. K. Thompson and U. Sakaguchi, *Inorg. Chem.*, 1998, **37**, 1028; (*c*) H. Okawa, T. Tokii, Y. Muto and S. Kida, *Bull. Chem. Soc. Jpn.*, 1973, **46**, 2464.
18 C. J. O'Connor, D. P. Freyberg and E. Sinn, *Inorg. Chem.*, 1979, **18**, 1077.
19 S. L. Lambert, C. L. Spiro, R. R. Gagné and D. N. Hendrickson, *Inorg. Chem.*, 1982, **21**, 68.
20 I. Morgenstern-Badarau, M. Rerat, O. Kahn, J. Jaud and J. Galy, *Inorg. Chem.*, 1982, **21**, 3050.
21 Y. Journaux, O. Kahn, I. Morgenstern-Badarau, J. Galy, J. Jaud, A. Bencini and D. Gatteschi, *J. Am. Chem. Soc.*, 1985, **107**, 6305.
22 T. Aono, H. Wada, Y. Aratake, N. Matsumoto, H. Okawa and Y. Matsuda, *J. Chem. Soc.*, *Dalton Trans.*, 1996, 25.
23 J. Ribas, C. Diaz, R. Costa, J. Tercero, X. Solans, M. Font-Bardía and H. Stoeckli-Evans, *Inorg. Chem.*, 1998, **37**, 233.
24 *Comprehensive Coordination Chemistry*, eds. G. Wilkinson, R. D. Gillard and J. A. McCleverty, Pergamon, Oxford, 1987.
25 S. Mohanta, K. K. Nanda, L. K. Thompson, U. Flörke and K. Nag, *Inorg. Chem.*, 1998, **37**, 1465 and references therein.
26 B. A. Goodman and J. B. Raynor, *Adv. Inorg. Chem. Radiochem.*, 1978, **35**, 701.
27 E. I. Solomon, M. D. Lowery, D. E. Root and B. L. Hemming, *Adv. Chem. Ser.* 1995, **246**, 121.
28 V. Staemmler, F. Birkelbach and C. Krebs, Bochum, 1997.
29 F. Lloret, R. Ruiz, M. Julve, J. Fans, Y. Journaux, I. Castro and M. Verdaguer, *Chem. Mater.*, 1992, **4**, 1150.
30 C. C. Chao, *J. Magn. Reson.*, 1973, **10**, 1; R. P. Scaring, D. J. Hodgson and W. E. Hatfield, *Mol. Phys.*, 1978, **35**, 701.
31 A. Bencini and D. Gatteschi, *EPR of Exchange Coupled Systems*, Springer, Berlin, 1990.
32 L. K. Thompson, S. K. Mandal, S. S. Tandon, J. N. Bridson and M. K. Park, *Inorg. Chem.*, 1996, **35**, 3117.
33 K. K. Nanda, L. K. Thompson, J. N. Bridson and K. Nag, *J. Chem. Soc.*, *Chem. Commun.*, 1994, 1337.
34 K. Wieghardt, P. Chaudhuri, B. Nuber and J. Weiss, *Inorg. Chem.*, 1982, **21**, 3086.
35 S. Gallert, personal communication.
36 R. R. Gagné, C. L. Spiro, T. J. Smith, C. A. Hamann, W. R. Thies and A. K. Shiemke, *J. Am. Chem. Soc.*, 1981, **103**, 4073; F. Ullmann and K. Brittner, *Chem. Ber.*, 1909, **42**, 2539.
37 G. M. Sheldrick, SADABS, Universität Göttingen, 1994.
38 G. M. Sheldrick, SHELXTL PLUS, Siemens Analytical X-Ray Instruments, Madison, WI, 1990.

Paper a908426f